

## Broadband dielectric spectroscopy of human albumin solution at physiological temperatures

© Zh.A. Salnikova, A.A. Kononov, A.P. Smirnov, R.A. Kastro

Herzen State Pedagogical University of Russia, Institute of Physics, St. Petersburg, Russia

E-mail: jannete90@mail.ru

Received November 22, 2024

Revised February 20, 2025

Accepted February 24, 2025

The parameters of relaxation processes in human albumin solution were determined and analyzed by dielectric spectroscopy through the analysis of behavior of a complex electrical module in a wide frequency range 1 Hz–2 GHz and in the range of physiological temperatures 33 °C–42 °C. Three relaxation processes were discovered and based on their approximation via Havriliak–Negami equation for a complex electrical module their relaxation parameters  $\alpha$ ,  $\beta$ ,  $\tau_0$  were determined, the time distribution functions of relaxation oscillators  $G(\tau)$  were plotted, and their activation energies  $E_a$  were calculated. Assumptions are made regarding the identification of possible kinetic units responsible for these processes.

**Keywords:** complex electrical module, relaxation parameters, Havriliak–Negami equation, time distribution function of relaxation oscillators.

DOI: 10.61011/TP.2025.06.61388.427-24

### Introduction

Method of dielectric spectroscopy is widely used in the dielectrics physics, i.e. the studies of frequency dependencies of conductivity, permittivity and loss factor [1–3] at various temperatures. This method is used to study both synthetic polymers of various types [4–6] and biopolymers [7–9]. The method of dielectric spectroscopy makes it possible to relate the dielectric properties of the studied sample to the electrical properties of the molecules forming it, in particular, to their dipole moments, as well as to draw some conclusions about potentials of intramolecular rotations and intermolecular interactions [10–14]. When analyzing maxima on the loss factor frequency curve it is possible to find the relaxation parameters of dielectric materials, at that, the empiric Havriliak–Negami equation being often used. However, with high electrical conductivity, relaxation maxima cannot be detected based on the loss factor frequency curves. To detect them, it is advisable to use the method of a complex electrical module [15].

Human albumin is one of the main protein components of blood, contained in its serum and performing the functions of transporting various substances, as well as maintaining osmotic blood pressure. It makes about 55% of all proteins contained in the blood serum. In a day, the human body produces 10–15 g of albumin. The albumin molecule is a globular protein with a mass of about 67 kDa, consisting of a single polypeptide chain and 585 amino acid residues, the arrangement of which is represented, for example, in [16]. Albumin relates to the class of alpha-proteins. Its secondary structure consists of alpha helices (50%–68%) and beta-sheets (16%–18%), as well as a disordered part of the macromolecule [17]. Due to 17 disulfide bridges, a tertiary

structure is formed consisting of three domains, each of which consists of two subdomains containing 6 and 4 alpha helices, respectively. In this case, hydrophobic interactions between the domains form the globular structure of the albumin molecule. The hydrodynamic radius of albumin molecules in an aqueous solution is 4.2 nm [18], and the conformation may be represented as an asymmetrical flattened ellipsoid [19]. The albumin molecule contains about a hundred pairs of positive and negative amino acid residues (99 positive and 126 negative [20]). In this case, the dipole moment of the albumin molecule is about 500 D [21], which determines its electrical properties in solution. Generalized information about albumin is presented in [22].

The purpose of this work is to study the dielectric properties of human serum albumin solution at physiological temperatures in a wide range of frequencies. By analyzing the behavior of frequency dependences of the real and imaginary components of the complex electrical module, it was possible to detect relaxation maxima, the study of which made it possible to determine the relaxation parameters  $\alpha$ ,  $\beta$ ,  $\tau_0$  and based on them to construct a function for the time distribution of relaxation oscillators and calculate the activation energy of the detected processes. Since human albumin is one of the main proteins of his blood serum, when analyzing the values of relaxation parameters  $\alpha$ ,  $\beta$ ,  $\tau_0$  of blood serum samples, the contribution of the corresponding relaxation parameters of albumin can be identified. This may be relevant in the analysis of relaxation parameters of blood serum from healthy donors and sick patients and may be of interest in the analysis of disease development, as well as in the development of medicines for the treatment of sick patients.

## 1. Calculation of dielectric spectra

### 1.1. Relaxation equations

To analyze the relaxation properties of dielectrics, the concept of complex permittivity  $\varepsilon^*(f)$  is used, which is determined by the expression:  $\varepsilon^*(f) = \varepsilon'(f) - i\varepsilon''(f)$ , where  $f$  is the frequency of the applied electric field,  $\varepsilon'(f)$  is the real part of the complex permittivity, which is called the permittivity of the medium and characterizes the degree of shielding of the external electric field,  $\varepsilon''(f)$  — the imaginary part of the complex dielectric permittivity, which is called the dielectric loss factor and characterizes the absorption of energy and its transformation into a thermal form. Values  $\varepsilon'(f)$  and  $\varepsilon''(f)$  are defined experimentally by means of dielectric spectrometers.

In general, the processes of dielectric relaxation are expressed as Havriliak–Negami (HN) equation [23]:

$$\varepsilon^*(\omega) = \varepsilon_\infty + \frac{\varepsilon_s - \varepsilon_\infty}{(1 + (i\omega\tau_0)^{1-\alpha})^{1-\beta}}, \quad (1)$$

where  $\varepsilon_s$ ,  $\varepsilon_\infty$  — static and high-frequency permittivity  $\varepsilon'(f)$  ( $\varepsilon_s$  — at  $f \rightarrow 0$ ,  $\varepsilon_\infty$  — at  $f \rightarrow \infty$ ),  $\omega = 2\pi f$  — cyclic frequency,  $\tau_0$  — the most probable relaxation time of kinetic units of the sample (molecules, their individual parts, as well as molecular complexes),  $\alpha$  — width of relaxation spectrum,  $\beta$  — dissymmetry of this spectrum. These parameters vary within the following intervals:  $0 \leq \alpha < 1$ ,  $0 \leq \beta < 1$ . The larger the value  $\alpha$ , the greater the frequency variance of relaxation times of the kinetic units of sample  $\tau$  relative to  $\tau_0$ , i.e., the wider the relaxation spectrum, therefore it is advisable to use the value  $1-\alpha$  in the formula; the greater  $\beta$ , the greater is its dissymmetry, i.e., the degree of deviation of the spectrum from its symmetry, therefore, it is advisable to use the value  $1-\beta$  in the formula. For Debye spectrum  $\alpha = 0$ ,  $\beta = 0$ .

Parameters  $\alpha$ ,  $\beta$ ,  $\tau_0$  are the basic relaxation parameters of the studied object.

The theoretical description of dielectric relaxation of the sample's kinetic units, considered as independent dipoles with several discrete orientation states, implies the presence of dipoles with different relaxation times  $\tau$  [24]. The cooperative nature of re-orientation of the molecule considered as a dipole implies its single step-like turns under the action of external field, when the probability of its re-orientation and energy activation depend on the orientation of neighbors, which, in its turn leads to emergence of the relaxation time spectrum [25], characterized by  $G(\tau)$  function of relaxation time distribution of kinetic units of  $\tau$  sample relative to  $\tau_0$ . The analytical expression for the function  $G(\tau)$  can be represented as [26]:

$$G(\tau) = \frac{(\tau/\tau_0)^{(1-\alpha)(1-\beta)} \sin((1-\beta)\theta)}{\pi\tau [(\tau/\tau_0)^{2(1-\alpha)} + 2(\tau/\tau_0)^{(1-\alpha)} \cos(\pi(1-\alpha)) + 1]^{\frac{1-\beta}{2}}}, \quad (2)$$

where

$$\theta = \arctg \left[ \frac{\sin(\pi(1-\alpha))}{(\tau/\tau_0)^{(1-\alpha)} + \cos(\pi(1-\alpha))} \right], \quad 0 \leq \theta \leq \pi.$$

The half-width of the function  $G(\tau)$  is determined by the parameter  $\alpha$ , and its dissymmetry by the parameter  $\beta$ . The larger these parameters are, the broader and more dissymmetric the function  $G(\tau)$  is.

At  $\alpha = 0$  and  $\beta = 0$  the HN equation transforms into Debye equation [27]:

$$\varepsilon^*(\omega) = \varepsilon_\infty + \frac{\varepsilon_s - \varepsilon_\infty}{1 + i\omega\tau_0}. \quad (3)$$

In this case,  $G(\tau)$  is a delta function of  $\delta(\tau_0)$  [3], which corresponds to the state where all kinetic units of the sample have the same relaxation time  $\tau_0$ .

At  $\alpha \neq 0$  and  $\beta = 0$  the HN equation is transformed into Cole–Cole equation [28]:

$$\varepsilon^*(\omega) = \varepsilon_\infty + \frac{\varepsilon_s - \varepsilon_\infty}{1 + (i\omega\tau_0)^{1-\alpha}}. \quad (4)$$

In this case,  $G(\tau)$  is a symmetric function relative to  $\tau_0$  [3] and its half-width is determined by the parameter  $\alpha$ .

At  $\alpha = 0$  and  $\beta \neq 0$  the HN equation is transformed into Davidson–Cole equation [29]:

$$\varepsilon^*(\omega) = \varepsilon_\infty + \frac{\varepsilon_s - \varepsilon_\infty}{(1 + i\omega\tau_0)^{1-\beta}}. \quad (5)$$

In this case,  $G(\tau)$  is a dissymmetric function relative to  $\tau_0$  [3] and its dissymmetry is determined by the parameter  $\beta$ .

The parameters  $\alpha$ ,  $\beta$ ,  $\tau_0$  and the function  $G(\tau)$  can be determined if there are relaxation maxima based on the experimentally obtained dependence  $\varepsilon''(f)$ . If these relaxation maxima cannot be detected (as in our case), then the determination of these parameters by this method becomes impossible. In view of this, we applied the method of analyzing the real and imaginary components of a complex electrical module, which was previously used for dielectric studies of blood serum in various oncological diseases [30], chronic lymphocytic leukemia [31,32], Ehrlich's carcinoma [33], oncohematological diseases [34], as well as for a synthetic polymer based on amide (in biophysics — peptide) groups — polyamide SPA-3 [35], which is a good model of intramolecular movements in peptide groups of biopolymers.

### 1.2. Complex electrical module method

Complex electrical module  $M^*(\omega)$  is a reciprocal of the complex permittivity that is defined as follows

$$M^*(\omega) = M'(\omega) + iM''(\omega).$$

$M'(\omega)$ ,  $M''(\omega)$  are the real and imaginary components of the complex electrical module, respectively. They are equal

$$M'(\omega) = \frac{\varepsilon'(\omega)}{\varepsilon'^2(\omega) + \varepsilon''^2(\omega)}, \quad (6)$$

$$M''(\omega) = \frac{\varepsilon''(\omega)}{\varepsilon'^2(\omega) + \varepsilon''^2(\omega)}. \quad (7)$$

From HN (1) equation we may mathematically derive the theoretical equations for  $M'(\omega)$  and  $M''(\omega)$  [36]:

$$M'(\omega) = \frac{A^{1-\beta} M_\infty M_s [A^{1-\beta} M_s + (M_\infty - M_s) \cos(1-\beta)\varphi]}{A^{2(1-\beta)} M_s^2 + 2A^{1-\beta} M_s (M_\infty - M_s) \cos(1-\beta)\varphi + (M_\infty - M_s)^2}, \quad (8)$$

$$M''(\omega) = \frac{A^{1-\beta} M_\infty M_s (M_\infty - M_s) \sin(1-\beta)\varphi}{A^{2(1-\beta)} M_s^2 + 2A^{1-\beta} (M_\infty - M_s) M_s \cos(1-\beta)\varphi + (M_\infty - M_s)^2}, \quad (9)$$

where

$$M_\infty = \frac{1}{\varepsilon_\infty}, \quad M_s = \frac{1}{\varepsilon_s},$$

$$A = \left[ 1 + 2(\omega\tau_0)^{1-\alpha} \sin \frac{\pi\alpha}{2} + (\omega\tau_0)^{2(1-\alpha)} \right]^{1/2},$$

$$\varphi = \arctg \left[ \frac{(\omega\tau_0)^{1-\alpha} \cos \frac{\pi\alpha}{2}}{1 + (\omega\tau_0)^{1-\alpha} \sin \frac{\pi\alpha}{2}} \right].$$

It should be noted that parameters  $\varepsilon_s$ ,  $\varepsilon_\infty\omega$ , and  $\alpha, \beta, \tau_0$  — have the same physical sense as equation (1).

$\varepsilon'(f)$  and  $\varepsilon''(f)$ , as a rule, are values that can be measured in the experiment. According to the formulas (6), (7), the dependencies  $M'(\omega)$ ,  $M''(\omega)$  are plotted and their subsequent approximation using formulas (8) and (9) is made. The least squares method is used to plot the approximating curves. The relaxation parameters  $\alpha, \beta, \tau_0$  are defined empirically from the principle of the best simultaneous approximation of  $M''(\omega)$ ,  $M'(\omega)$ ,  $M''(M')$  curves.

## 2. Experiment procedure

### 2.1. Samples

The experimental samples were human albumin 20% sold in RF pharmacy chain, produced by Baxter AG, Austria. Sample composition: human albumin — 200 g/L; sodium chloride — 3 g/L; sodium caprylate — 2.7 g/L; sodium acetyltryptophan — 4.3 g/L; water for injection — up to 11. General content of sodium 100–130 mmol/L.

### 2.2. Equipment and measurement procedure

The dielectric spectra were measured using spectrometer Novocontrol Concept 81 of the collective use center in Herzen State Pedagogical University of Russia [37] within the frequency band  $f = 1-2 \cdot 10^9$  Hz, and temperature interval 33 °C–42 °C. In the low frequency band  $f = 1-3 \cdot 10^6$  Hz the measurements were made by „voltmeter–ammeter“ method, and in high frequency area  $f = 3 \cdot 10^6-2 \cdot 10^9$  Hz the measurements were made by a MW method with a coaxial system.

In „voltmeter–ammeter“ method, an alternating voltage  $U_0(\omega)$  from the generator is supplied to the measured sample and the current passing through it is measured:

$$I^*(\omega) = I_a(\omega) + i I_p(\omega),$$

where  $I_a(\omega)$  and  $I_p(\omega)$  — active and reactive components of the current. Complex impedance  $Z^*(\omega)$  is calculated by formula

$$Z^*(\omega) = Z'(\omega) + i Z''(\omega) = \frac{U_0(\omega)}{I^*(\omega)},$$

Capacitance  $C(\omega)$  and electric conductivity  $\sigma'(\omega)$  of the sample are found from the formula

$$Z'(\omega) + i Z''(\omega) = \frac{1}{\sigma'(\omega)} + \frac{1}{i\omega C(\omega)}.$$

The dielectric constant  $\varepsilon'(\omega)$  is calculated using the formula of a flat capacitor

$$C(\omega) = \frac{\varepsilon'(\omega)\varepsilon_0 S}{d}.$$

The loss factor  $\varepsilon''(\omega)$  is found from the formula

$$\varepsilon''(\omega) = \varepsilon'(\omega) \operatorname{tg} \delta(\omega),$$

where

$$\operatorname{tg} \delta(\omega) = \frac{I_a(\omega)}{I_p(\omega)}$$

— tangent of the dielectric loss angle.

In the microwave method, an electromagnetic wave is applied to the measured sample, and the complex reflection coefficient  $r^*(l)$  is measured. Complex impedance  $Z_s^*(\omega)$  is calculated by formula

$$Z_s^*(\omega) = Z_0 \frac{1 + r^*(l)}{1 - r^*(l)},$$

where  $Z_0$  — input resistance of the waveguide  $l$  long. Based on  $Z_s^*(\omega)$  all required parameters are found:  $C(\omega)$ ,  $\operatorname{tg} \delta(\omega)$ ,  $\varepsilon'(\omega)$ ,  $\varepsilon''(\omega)$ ,  $\sigma'(\omega)$ . The accuracy of impedance determination was 0.1%. The measurements were made using BDS 1308 cell (Novocontrol Technologies GmbH & Co) designed for operation with liquids.

WinDeta software (Novocontrol Technologies GmbH, Germany) was used to collect and display the measurement results.

The relaxation parameters  $\alpha, \beta, \tau_0$ , as well as relaxation time distribution function  $G(\tau)$  for kinetic units was defined by approximation of experimental curves  $M'(\omega)$  (6),  $M''(\omega)$  (7),  $M''(M')$  in HN equation for electrical module with the use of WinFit (Novocontrol Technologies GmbH & Co) software for approximation of  $M'(\omega)$  and  $M''(\omega)$  in equations (8) and (9) by the least-square method.

Approximation error for parameters  $\alpha, \beta$  didn't exceed 0.02; for parameter  $\tau_0$  it was no higher than 10%. When  $\alpha, \beta$  are about 0.0 their error didn't exceed 0.01.

Values of relaxation parameters  $\alpha$ ,  $\beta$ ,  $\tau_0$  (in compliance with equation (1))\*

$T, ^\circ\text{C}$	First relaxation process: $f = 10^1 - 10^2 \text{ Hz}$			Second relaxation process: $f = 10^4 - 10^5 \text{ Hz}$			Third relaxation process: $f = 10^8 - 10^9 \text{ Hz}$		
	$\alpha_1$	$\beta_1$	$\tau_{0,1} (s)$	$\alpha_2$	$\beta_2$	$\tau_{0,2} (s)$	$\alpha_3$	$\beta_3$	$\tau_{0,3} (s)$
33	0.09	0.62	$3.7 \cdot 10^{-2}$	0.35	0.02	$5.7 \cdot 10^{-6}$	0.00	0.37	$9.80 \cdot 10^{-10}$
34	0.05	0.73	$4.5 \cdot 10^{-2}$	0.32	0.00	$5.7 \cdot 10^{-6}$	0.00	0.35	$9.81 \cdot 10^{-10}$
35	0.03	0.74	$3.4 \cdot 10^{-2}$	0.31	0.01	$5.6 \cdot 10^{-6}$	0.00	0.38	$9.77 \cdot 10^{-10}$
36	0.02	0.74	$2.6 \cdot 10^{-2}$	0.30	0.03	$5.3 \cdot 10^{-6}$	0.00	0.38	$9.73 \cdot 10^{-10}$
37	0.00	0.74	$2.1 \cdot 10^{-2}$	0.30	0.02	$5.1 \cdot 10^{-6}$	0.00	0.30	$9.74 \cdot 10^{-10}$
38	0.04	0.72	$1.6 \cdot 10^{-2}$	0.29	0.05	$5.1 \cdot 10^{-6}$	0.00	0.34	$9.65 \cdot 10^{-10}$
39	0.09	0.70	$1.6 \cdot 10^{-2}$	0.29	0.07	$5.1 \cdot 10^{-6}$	0.00	0.35	$9.65 \cdot 10^{-10}$
40	0.30	0.43	$9.1 \cdot 10^{-3}$	0.32	0.07	$5.2 \cdot 10^{-6}$	0.00	0.35	$9.60 \cdot 10^{-10}$
41	0.28	0.41	$7 \cdot 9 \cdot 10^{-3}$	0.33	0.09	$5.2 \cdot 10^{-6}$	0.00	0.32	$9.59 \cdot 10^{-10}$
42	0.28	0.40	$6.9 \cdot 10^{-3}$	0.34	0.08	$5.2 \cdot 10^{-6}$	0.00	0.31	$9.56 \cdot 10^{-10}$

Note. \* — approximation error for parameters  $\alpha, \beta$  didn't exceed 0.02; for parameter  $\tau_0$  it didn't exceed 10%. With the values  $\alpha, \beta$  about 0.0 their error didn't exceed 0.01.

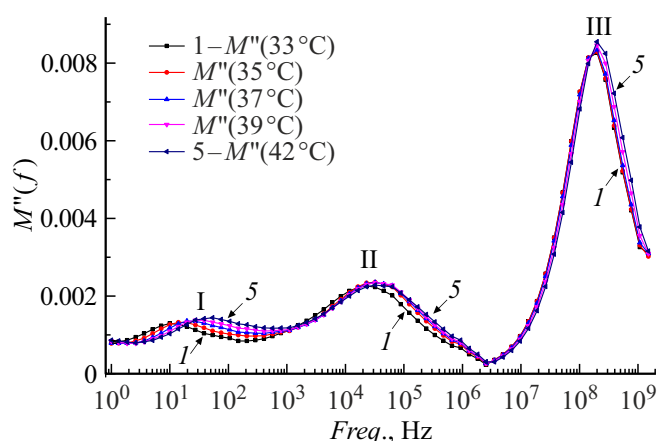


**Figure 1.** Frequency dependence of the imaginary part of the electrical module  $M''(f)$  at temperatures  $33^\circ\text{C}$ – $42^\circ\text{C}$ .

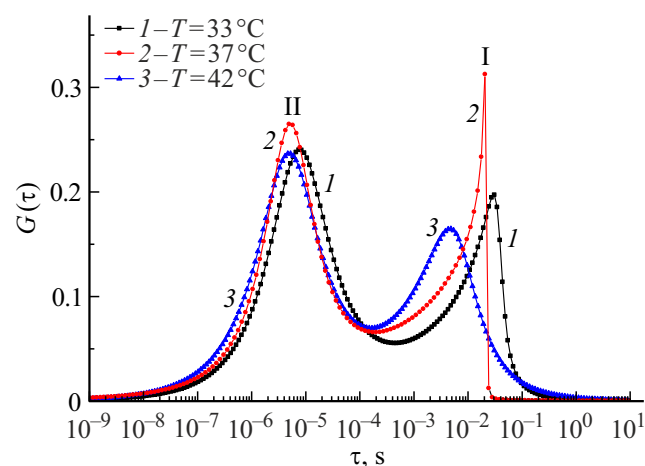


**Figure 2.** Relaxation oscillators time distribution function  $G(\tau)$  for the first (I) and the second (II) relaxation processes at different temperatures: 1 —  $33^\circ\text{C}$ , 2 —  $37^\circ\text{C}$ , 3 —  $42^\circ\text{C}$ .

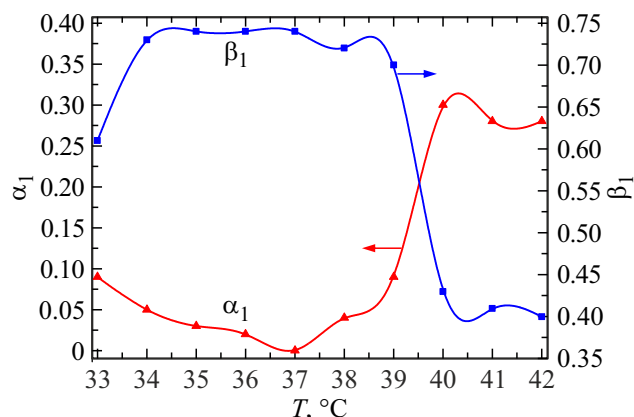
### 3. Results and discussion

Fig. 1 illustrates frequency dependencies  $M''(f)$  at temperatures  $33^\circ\text{C}$ – $42^\circ\text{C}$ . Three maxima were observed in these curves: the first one at  $f = 10^1 - 10^2 \text{ Hz}$ , the second one at  $f = 10^4 - 10^5 \text{ Hz}$ , the third one at  $f = 10^8 - 10^9 \text{ Hz}$ . For all maxima, the parameters  $\alpha, \beta, \tau_0$  were determined using HN equation for an electrical module using the WinFit program, according to the methodology described in sec. 2.2. The results of calculations of these relaxation parameters are presented in the following table.

The shift of the maxima  $M''(f)$  to the high frequency range with increasing temperature indicates the presence of three relaxation processes. In this case, the first and second processes partially overlap. The first process ends

at frequency  $f \sim 10^3 \text{ Hz}$  (Fig. 1), however  $M''(f) \neq 0$ , i.e. the second relaxation process starts. Fig. 2 illustrates the function of time distribution of relaxation oscillators  $G(\tau)$  for the first and second relaxation processes, plotted based on equation (2) in WinFit program.

It can be seen that the first and second relaxation processes do partially overlap. It should be noted that the degree of dissymmetry  $G(\tau)$  of the first relaxation process is determined by the large value of the parameter  $\beta_1$  ( $\beta_1 \approx 0.7$ ), and the half-width  $G(\tau)$  of the second relaxation process is determined by the large value of the parameter  $\alpha_2$  ( $\alpha_2 \approx 0.3$ ). Let's review each relaxation process in detail.



**Figure 3.** Temperature dependences of relaxation parameters  $\alpha_1(T)$  and  $\beta_1(T)$  of the first relaxation process.

### 3.1. First relaxation process

The first relaxation process corresponding to the maximum  $M''(f) \approx 1.5 \cdot 10^{-3}$  is observed at temperatures  $T = 33^\circ\text{C} - 42^\circ\text{C}$  in the frequency band  $f = 10^1 - 10^2$  Hz (Fig. 1). In the temperature range  $T = 33^\circ\text{C} - 9^\circ\text{C}$  this process is well described by Davidson–Cole equation (5), since  $\alpha_1 \approx 0$  and  $\beta_1 \approx 0.7$ .

Figure 3 shows the temperature dependences of the relaxation parameters  $\alpha_1(T)$ ,  $\beta_1(T)$  for this process.

In Fig. 3 at  $37^\circ\text{C}$  the minimum  $\alpha_1$  is clearly seen, as well as in the temperature range  $35^\circ\text{C} - 37^\circ\text{C}$  — the maximum  $\beta_1$  is observed. The decrease in parameter  $\alpha_1$  is probably due to the fact that the sizes of kinetic units become less different from each other. This conclusion can be drawn based on the fact that for Debye spectrum  $\alpha = 0$ , even in this case, the kinetic units in the system have almost the same size. Higher parameter  $\beta$  means that the spectrum becomes less symmetrical, since for Debye spectrum  $\beta = 0$ , even in this case, the kinetic units in the system have an identical shape. The very high value of  $\beta \sim 0.7$  in particular means that the shapes of kinetic units are significantly different. Thus, a simultaneous decrease in parameters  $\alpha$  and increase in  $\beta$  may be associated with a change in the conformation of the kinetic units of the first relaxation process.

Within the temperature range  $39^\circ\text{C} - 40^\circ\text{C}$  parameters  $\alpha_1$  and  $\beta_1$  are simultaneously significantly increasing: parameter  $\alpha_1$  rises threefold from 0.1 to 0.3, and parameter  $\beta_1$  decreases almost twofold from 0.7 to 0.42. These changes can also be explained by a change in the conformation of kinetic units of the first relaxation process. With a further increase in temperatures  $40^\circ\text{C} - 42^\circ\text{C}$  these parameters remain almost constant.

The equation [38] was used to calculate the activation energy of the dipole polarization process:

$$\tau_0 = A e^{E_a/kT}, \quad (10)$$

where  $A$  — constant for this liquid,  $E_a$  — activation energy,  $k$  — Boltzmann constant,  $T$  — temperature, [ $^\circ\text{K}$ ].

As a result, the following equation is obtained after taking the logarithm of equation (10):

$$\ln \tau_0 = \ln A + \frac{E_a}{kT}.$$

In its turn, after introducing the values:  $y = \ln \tau_0$ ,  $x = 1000/T$ ,  $\ln A = C$ , we have a straight line equation:

$$y = C + \frac{E_a}{1000k} x. \quad (11)$$

After constructing this straight line in the Cartesian coordinate system based on the data  $\tau_{0,1}$ ,  $T$  from the table, we determined the activation energy  $E_a$  using the following formula:

$$\text{tg } \alpha = \frac{E_a}{1000k}, \quad (12)$$

where  $\alpha$  — the straight line inclination angle (11).

Fig. 4 shows the curve of  $\ln \tau_{0,1}$  versus  $(1000/T)$  for the first process. The activation energy of the first relaxation process turned out to be equal  $E_{0,1} = (1.8 \pm 0.1)$  eV, i.e.  $(173 \pm 13)$  kJ/mol.

Since both the relaxation time and the activation energy turned out to be quite large ( $\tau_{0,1} = 6.9 \cdot 10^{-3} - 3.7 \cdot 10^{-2}$  s,  $E_a = 173$  kJ/mol), respectively, the possible kinetic units of the first process include whole albumin molecules, or large segments, for example, domains that make up their tertiary structure. In both cases, the first relaxation process is a dipole-segmental motion, or a process [6] associated with orientation rotations of large segments of albumin macromolecules, or with a change in albumin molecule conformation as a whole.

The change in conformation of albumin molecule at physiological temperatures as a first-order phase transition of „globule–tangle“ was shown in the work of E.B. Shadrin group [39]. In this work, it was noted that the temperature of the phase transition depends on concentration of an aqueous solution of albumin and at a concentration of 5%

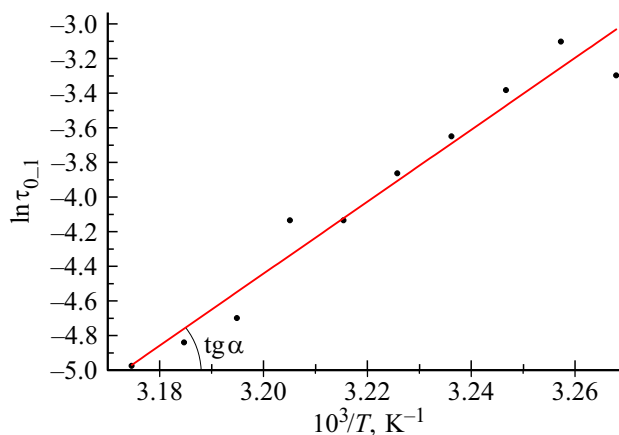


**Figure 4.** Temperature dependence of the relaxation time  $\tau_{0,1}$  for the first relaxation process:  $\ln \tau_{0,1}$  ( $1000/T$ ).

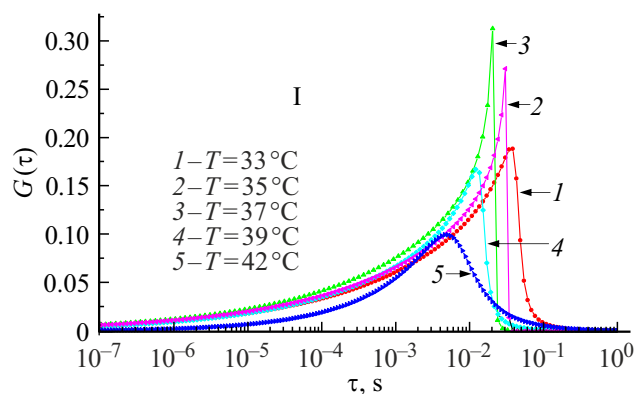


**Figure 5.** Relaxation oscillators time distribution function  $G(\tau)$  for the first relaxation process at different temperatures: 1 — 33°C, 2 — 35°C, 3 — 37°C, 4 — 39°C, 5 — 42°C.

makes 38°C. According to these data, the phase transition temperature decreases with increasing concentration. In our case (concentration of albumin in water 20%) at a temperature of 37°C we observe the minimum  $\alpha_1 = 0$  and maximum  $\beta_1 = 0.74$ . Thus, the minimum of parameter  $\alpha_1$ , equal to zero, with the simultaneous maximum of parameter  $\beta_1$ , may be an indicator of a phase transition of the first kind. It should be stressed that within the temperature range 39°C–40°C a simultaneous drastic change of parameters  $\alpha_1$  and  $\beta_1$  is observed;  $\alpha_1$  increases threefold, and  $\beta_1$  decreases almost twofold (fig. 3). At higher temperatures, the parameters  $\alpha_1$  and  $\beta_1$  change slightly.

Separation of function  $G(\tau)$  (Fig. 2) in first and second processes is illustrated in Fig. 5 and in section. 3.2, respectively.

The function  $G(\tau)$  shown in Fig. 5 for the first relaxation process in the temperature range  $T = 33^\circ\text{C}–39^\circ\text{C}$  is clearly dissymmetrical, which is confirmed by the value of parameter  $\beta_1 = 0.61–0.74$ , and at the same time it is very wide (7 frequency orders  $10^{-8}–10^{-1}$  s). At higher temperatures,  $G(\tau)$  becomes more symmetrical, which is confirmed by the value of parameter  $\beta_1 = 0.4$  and less wide (5 frequency orders  $10^{-6}–10^{-1}$  s). Function  $G(\tau)$  reaches its maximum  $T = 37^\circ\text{C}$ , being the most dissymmetrical. Maximum  $G(\tau)$  at  $T = 37^\circ\text{C}$  lies within  $\tau_{0,1} = 2.1 \cdot 10^{-2}$  s, at that, the relaxation oscillators are present from  $\tau$  up to  $10^{-8}$  s (6 of frequency orders relative  $\tau_{0,1}$ ), but there are no relaxation oscillators from  $\tau > 6 \cdot 10^{-2}$  s (below 1/2 of the frequency order relative to  $\tau_{0,1}$ ). This distribution of relaxation oscillators can be explained by the fact that there is a superposition of movements of the skeleton of the albumin molecule main chain and internal rotations in the lateral polar groups strongly linked to the main chain of the molecule. A single process may be observed at such movements [40], and  $G(\tau)$  function becomes significantly dissymmetrical [40].

### 3.2. Second relaxation process

The second relaxation process corresponding to the maximum  $M''(f) \approx 2 \cdot 10^{-3}$  is observed at temperatures  $T = 33^\circ\text{C}–42^\circ\text{C}$  in the frequency band  $f = (10^4–10^5)$  Hz (Fig. 1). With an increase in temperature, a shift of the maximum  $M''$  to the high frequency range is observed, which indicates a relaxation process associated with orientation rotations of kinetic units of albumin macromolecules. However, this shift is a way lower than in the first process. In the temperature range  $T = 33^\circ\text{C}–42^\circ\text{C}$  this process is well described by Cole–Cole equation (4), since in this case  $\alpha_2 \approx 0.3$  and  $\beta_2 \approx 0$ .

Figure 6 shows the temperature dependences of relaxation parameters  $\alpha_2(T)$ ,  $\beta_2(T)$  for the second process.

Unlike the first process, the second process has a very wide ( $\alpha_2 \sim 0.3$ ) but symmetric ( $\beta_2 < 0.1$ ) relaxation spectrum. At temperatures 38°C–39°C the parameter  $\alpha_2$  is minimal, the parameter  $\beta_2$  increases monotonously in the temperature range 34°C–41°C. The average relaxation time for the second process is almost four orders of magnitude shorter than for the first ( $\tau_{0,2} \sim 5 \cdot 10^{-6}$  s and  $\tau_{0,1} \sim 2 \cdot 10^{-2}$  s, respectively), which indicates different sizes and masses of the corresponding kinetic units of these processes.

The equations (10)–(12) were also used to calculate the activation energy of the second process. Fig.7 shows the function of  $\ln \tau_{0,2}$  versus  $(1000/T)$ .

The activation energy of the second relaxation process turned out to be equal  $E_{a,2} = (0.10 \pm 0.02)$  eV, i.e.  $9 \pm 2$  kJ/mol.

Since the activation energy of the second process is significantly less compared to the first one and the relaxation times of the second process are also significantly less than the first one, the alpha helices of albumin molecules (dipole group motion, or  $\beta$  process) may possibly represent themselves the kinetic units of the second process [6]. At the same time, due to thermal fluctuations, the angles of internal rotation in the main ( $\varphi_i, \psi_i, \omega_i$ ) and lateral ( $\chi_i$ )

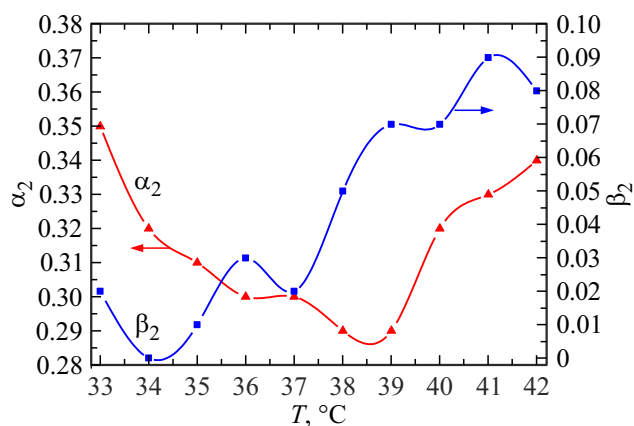


**Figure 6.** Temperature dependences of relaxation parameters  $\alpha_2(T)$  and  $\beta_2(T)$  of the second relaxation process.

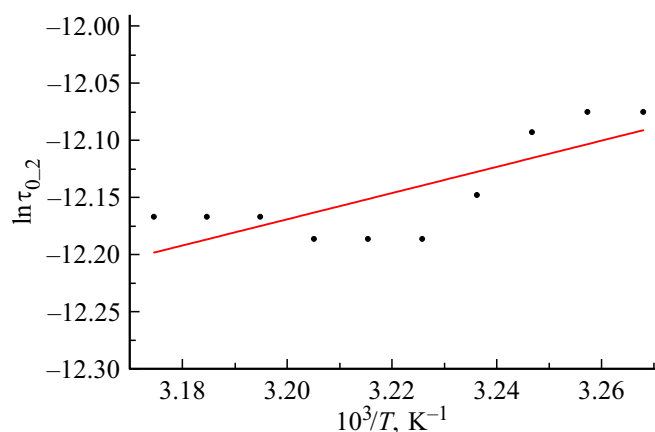


**Figure 7.** Temperature dependence of the relaxation time  $\tau_{0,2}$  for the second relaxation process:  $\ln \tau_{0,2} (1000/T)$ .

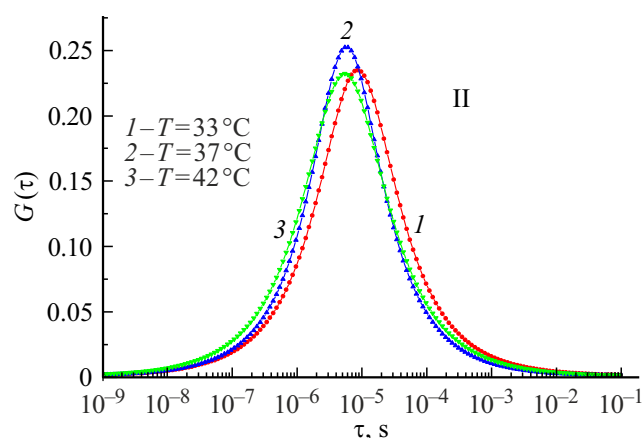


**Figure 8.** Relaxation oscillators time distribution function  $G(\tau)$  for the second relaxation process at different temperatures: 1 — 33 °C, 2 — 37 °C, 3 — 42 °C.

chains may vary [41]. The presence of three rotation angles expands the relaxation spectrum, i.e., increases the parameter  $\alpha_2$ . However, the relaxation spectrum is symmetrical ( $\beta_2 < 0.1$ ). This suggests that the angles of internal rotation can equally increase or decrease.

Function  $G(\tau)$  for the second process is given in Fig. 8.

For the second process, the function  $G(\tau)$  is also very wide (6 frequency orders ( $10^{-8}$ – $10^{-2}$  s), but symmetrical, which is confirmed by the value of the parameter  $\beta_2 < 0.1$ . Compared to the first relaxation process (Fig. 5), the half-width  $G(\tau)$  for the second process is a way larger. Since parameter  $\alpha_2 \approx 0.3$  and function  $G(\tau)$  are wide for the second relaxation process, a wide range of different-scale movements with different activation barriers and different characteristic times may occur in the albumin molecule, which is a common property of proteins and can be described as a set of dielectric permittivity, each of which corresponds to its time interval [42].

### 3.3. Third relaxation process

The third relaxation process corresponding to the maximum  $M''(f) \approx 8 \cdot 10^{-3}$  is observed at temperatures  $T = 33$  °C–42 °C in the frequency range of  $f = (10^8$ – $10^9)$  Hz. This process is well described by Davidson–Cole equation (5), since in this case  $\alpha_3 = 0$  and  $\beta_3 \neq 0$  in the whole temperature range.

Figure 9 shows the temperature dependences of relaxation parameters  $\alpha_3(T)$ ,  $\beta_3(T)$  for the third process.

It can be seen that with increasing temperature, the parameter  $\beta_3$  decreases, while a minimum is observed at 37 °C. This means that the system shows a weak tendency to symmetry, although it remains rather asymmetrical ( $\beta_3 > 0.3$ ). In turn, the parameter  $\alpha_3 = 0$  over the entire temperature range 33 °C–42 °C. This means that the system has a minimally wide relaxation spectrum (for Debye spectrum  $\alpha_3 = 0$ ).

Fig. 10 shows the function  $G(\tau)$  for the third relaxation process, plotted using the equation (2) in WinFit program at  $T = 38$  °C. For cases of other temperatures, it looks similar.

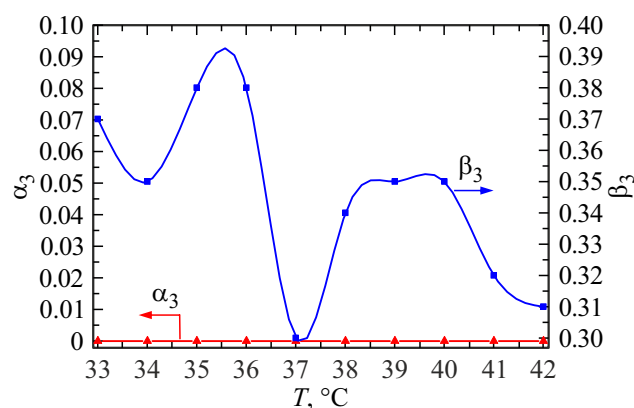


**Figure 9.** Temperature dependences of relaxation parameters  $\alpha_3(T)$  and  $\beta_3(T)$  of the third relaxation process.

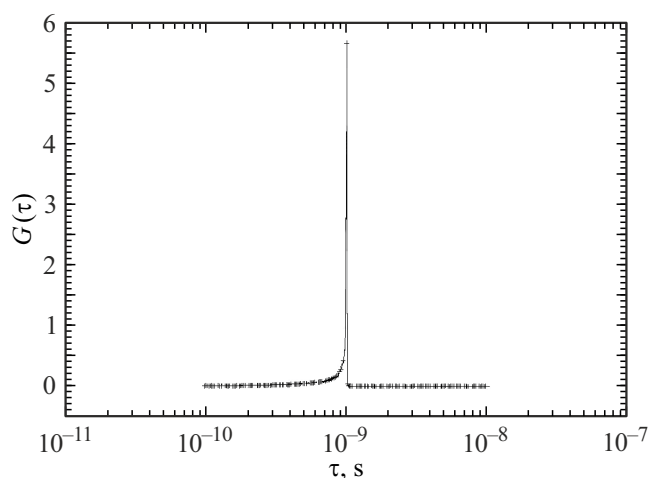


**Figure 10.** Relaxation oscillators time distribution function  $G(\tau)$  for the third relaxation process at a temperature 38 °C.

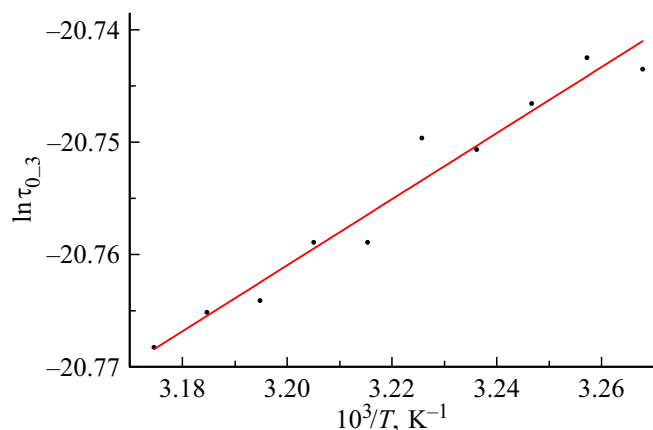


**Figure 11.** Temperature dependence of the relaxation time  $\tau_{0,3}$  for the third relaxation process:  $\ln \tau_{0,3} (1000/T)$ .

This function has practically no half-width, but there is a dissymmetry, which is confirmed by the parameter  $\beta_3$  ( $\beta_3 \approx 0.3$ ).

To calculate the activation energy of the third process also equations (10)–(12) were used. Fig. 11 shows the dependence  $\ln \tau_{0,3}$  on  $(1000/T)$ . The activation energy of the third relaxation process turned out to be equal  $E_{a,3} = (0.025 \pm 0.002)$  eV, i.e.  $(2.4 \pm 0.2)$  kJ/mol.

The average relaxation time of kinetic units of the third process obtained by us is  $\tau_{0,3} \sim 1 \cdot 10^{-9}$  s. As the temperature rises, there is a slight shift of the maximum  $M''$  to the high frequency range, which is a way lower than in the first and second processes. This shift is related to the orientation rotations of kinetic units of various shapes ( $\beta \sim 0.3$ ). Most likely, such units are the polar amino acid residues of the main chain of the albumin molecule. As mentioned in the abstract of this article, there are about two hundred (99 positive and 126 negative) units.

### 3.4. Activation energies of three processes compared

Let's compare the activation energies of the three relaxation processes:  $E_{a,1} = 173$  kJ/mol;  $E_{a,2} = 9$  kJ/mol;  $E_{a,3} = 2.4$  kJ/mol.

The maximum activation energy  $E_{a,1}$  and the longest relaxation time ( $\tau_{0,1} \sim 10^{-2}$  s) are observed in the first relaxation process. This is probably due to the size (radius of about 4.2 nm) and the shape of albumin molecules (an asymmetric flattened ellipsoid), since they determine the magnitude of its dipole moment (about 500 D) and, as a result, the energy of the dipole-dipole interaction between both albumin and water molecules, and between albumin molecules. It should be emphasized that the energy of van der Waals dipole-dipole interaction between molecules is proportional to the product of the squares of their dipole moments [12]. Since the albumin molecule is large in size and dipole moment, it will interact with a large number

of water molecules. Accordingly, there will be a large energy of dipole-dipole interaction of albumin and water molecules, as well as albumin molecules with each other. To overcome these energy barriers, a large activation energy is required  $E_{a,1}$ .

The activation energy of the second process  $E_{a,2}$  is 20 times less than that of the first one, i.e., the energy barriers of dipole rotations of alpha helices inside the albumin molecule as a whole is rotated in an aqueous environment. As mentioned in [43], proteins are characterized by low dielectric constant, the presence of a constant intra-protein electric field, and a wide range of dielectric relaxation times. It was the wide relaxation spectrum of the second process ( $\alpha_2 \approx 0.32$ ) that we observed.

The activation energy of the third process  $E_{a,3}$  is 4 times less than that of the second one and 72 times less compared to the first one. This means that the energy barriers of the dipole orientation of polar amino acid residues are significantly lower than the barriers of dipole rotations of alpha helices and much lower than the barriers of dipole rotations of whole albumin molecules. For the third process  $\alpha = 0$ ,  $\beta \approx 0.35$  which makes it similar to the first process ( $\alpha \approx 0$ ,  $\beta \approx 0.7$ ) and different from the second one ( $\alpha \approx 0.30$ ,  $\beta \approx 0.0$ ). This is probably due to the different shapes of amino acid residues and different values (and direction relative to the axis) of their dipole moments.

## Conclusion

During the study of a 20% aqueous solution of human serum albumin at physiological temperatures, three relaxation processes were detected and their parameters determined. Most likely, the first of them (low-frequency) well described at  $T = 33^\circ\text{C} - 39^\circ\text{C}$  by Davidson–Cole equation (5) is associated with rotations of whole albumin molecules under the action of an alternating electric field, as well as, possibly, with a change in the conformation of albumin molecules from globular to the tangle one at  $37^\circ\text{C}$ . The cooperative nature of the rotation of whole albumin molecules is characterized by high values of  $\beta_1$  and the activation energy  $E_{a,1}$ , as well as the shape of the function  $G(\tau)$  (Fig. 5). The second process (medium frequency), well described by the Cole–Cole equation (4) is probably related to the rotation of the alpha helices of albumin molecules. The third (high-frequency) process, well described by Davidson–Cole equation (5) is probably related to the rotations of the polar amino acid residues of the albumin backbone.

Analysis of graphs  $\alpha(T)$ ,  $\beta(T)$  can provide new information about the change in the conformation of kinetic units of this relaxation process, including phase transitions in them. The minimum of parameter  $\alpha$ , equal to zero, with the simultaneous maximum of parameter  $\beta$ , may be an indicator of a phase transition of the first kind.

The method of dielectric spectroscopy can be a good addition to other various methods of studying serum albumin in clinical medicine, since this method is able to effectively detect changes in the conformations of relaxers (structural units) of biopolymers, and therefore variations in intermolecular interactions in their aqueous solutions. Dielectric spectroscopy allows for a deeper understanding of the nature of relaxation processes in a wide class of complex liquids, including biological ones, which has not yet been sufficiently developed.

In conclusion, we should emphasize that the method of complex electrical module is effective for studying relaxation processes in aqueous solutions of polymers, including water-soluble globular proteins, the main molecules of wildlife.

### Conflict of interest

The authors declare that they have no conflict of interest.

### References

- [1] G.I. Scanavi. *Fizika dielektrikov (oblast' slablykh poley)* (GITTL, M.-L., 1949), 500 p.
- [2] N.P. Bogoroditsky, Yu.M. Volokobinsky, A.A. Vorobyev, B.M. Tareev. *Teoriya dielektrikov* (Energiya, M.-L., 1965), 344 p (in Russian).
- [3] F. Kremer, A. Schonhals. *Broadband Dielectric Spectroscopy* (Springer–Verlag, Berlin Heidelberg, 2003), 730 p.
- [4] B.I. Sazhin, *Elektricheskie svoistva polimerov* (Khimiya, L., 1986) 3d edition, 224 p.(in Russian).
- [5] E.R. Blythe, D. Bloor, *Electrical Properties of Polymers* (Fizmatlit, M, 2008), p.368.
- [6] Yu.A. Gorokhovatskii, E.A. Karulina, D.E. Temnov, *Fizika polimernykh dielektrikov* (Izd. RGPU, St. Petersburg, 2013) 124 p.(in Russian).
- [7] O. Schanne, P. Ruiz, E. Ceretti. *Impedance measurements in biological cell* (John Willey & Sons, 1978), 430 p.
- [8] *Dielectric Relaxation in Biological Systems: Physical Principles, Methods, and Applications*, ed. V. Raicu, Y. Feldman (Scholarship, Published to Oxford, 2015), 430 p.
- [9] A.N. Romanov, E.Yu. Vinokurova, A.O. Kovrigin, A.F. Lazarev, V.A. Lubennikov, N.A. Romanova, S.A. Komarov, *Dielektricheskie kharakteristiki biologicheskikh zhidkostei cheloveka pri razviti onkologicheskikh zabolevani (mikrovolnovyi diapazon)* (Barnaul, 2008) p.70 (in Russian).
- [10] S. Midzusima. *Structure of molecules and internal rotation* (Publ.house IL. M, 1957), 264 p.
- [11] *Internal molecular rotation*, revised by V.J. Orvill-Tomas, translated from English/Ed. by Yu.A. Pentin (Mir, M., 1977), 510 p.
- [12] I.G. Kaplan. *Vvedenie v teoriyu mezhmolekulyarnykh vzaimodeistviy* (Nauka, M., 1982), 312 p (in Russian).
- [13] *Mezhmolekulyarniye vzaimodeistviya: ot dvukhatomnykh molecul do biopolymerov*, rev.by B. Pul'man (Mir, M., 1981), 592 p (in Russian).
- [14] I.G. Kaplan. *Mezhmolekulyarniye vzaimodeistviya. Fizicheskaya interpretaciya, komp'yuternye raschety i model'nye potentsialy*, translated from English (BINOM, Laboratoriya znaniy, M., 2017), 394 p. (in Russian)
- [15] J.A. Salnikova, A.A. Kononov, A.P. Smirnov, R.A. Castro Arata. *Phys. Complex Systems*, **3**(1), 11 (2022). DOI: 10.33910/2687-153X-2022-3-1-11-20
- [16] *Albumin syvorotki krovi v klinicheskoy meditsine*, revised by Yu.A. Gryzunova, G.E. Dobretsova (Irius, M., 1994), 226 p. (in Russian).
- [17] Jr.T. Peters. *All About Albumin: Biochemistry, Genetics, and Medical Applications* (Academic Press, 1996), 432 p.
- [18] N.P. Malomuzh, A.V. Khorolsky. *Zhurn. fiz. khim.*, **95**(2), 231 (2021) (in Russian).
- [19] M.A. Kiselev, Yu.A. Gryzunov, G.E. Dobretsov, M.N. Komarova. *Biofizika*, **46**(3), 423 (2001) (in Russian).
- [20] A. Lenidzher. *Biokhimiya* (Mir, M., 1974, 958 p.)
- [21] V.V. Gibizova, I.A. Sergeeva, G.P. Petrova, A.V. Priezdev, N.G. Khlebtsov. *Vestnik Moskovskogo un-ta, Series 3. Physics. Astronomy. № 5 (Biophysics and medicine physics)*, 39 (2011).
- [22] Albumin. Electronic source. URL: [www.albumin.org](http://www.albumin.org) (date of access: 01.11.2024)
- [23] S. Havriliak, S. Negami. *J. Polymer Sci. Part C*, **14**(1), 99 (1966).
- [24] G. Frelikh. *Teoriya dielektrikov* (Publ.house IL. M 1960), 252 p (in Russian).
- [25] *Relaxatsionniye yavleniya v polymerakh*, rev.by G.M. Bartenev, Yu.V. Zelenev (Khimiya, L., 1972), 373 p. (in Russian)
- [26] S. Havriliak, S. Negami. *Polymer*, **8**, 161 (1967).
- [27] P. Debye, *Polar Molecules* (Chemical Catalog Company, Inc., 1931), 248 p.
- [28] K.S. Cole, R.H. Cole. *J. Chem. Phys.*, **9**, 341 (1941).
- [29] D.W. Davidson, R.H. Cole. *J. Chem. Phys.*, **18**, 1417 (1950); DOI: 10.1063/1.1747496
- [30] J.A. Salnikova, R.A. Castro. *VI St.Petersburg International Oncology Forum „Beliye nochi 2020“* (Thes.report 2020), p. 309.
- [31] Zh.A. Salnikova, L.V. Plotnikova, A.P. Smirnov A.D. Garifullin, A.Yu. Kuvshinov, S.V. Voloshin, A.M. Polyanichko. *AIP Conf. Proceed.* **2308**, 030018 (2020). DOI: 10.1063/5.0035270
- [32] J.A. Salnikova, L. V. Plotnikova, A.P. Smirnov, R.A. Castro, A.D. Garifullin, A.Yu. Kuvshinov, S.V. Voloshin, A. M. Polyanichko. *Materials of the 54-th school of PNPI on condensed matter physics* (SPb, 16-20.03.2020, [http://fks2020.pnpi.spb.ru/media/Sbornik\\_tez\\_FKS\\_2020\\_v\\_3.pdf](http://fks2020.pnpi.spb.ru/media/Sbornik_tez_FKS_2020_v_3.pdf) p. 157 (2020).
- [33] J.A. Salnikova, A.P. Smirnov, N.A. Verlov, R.A. Castro *ZhTF*, **92**(1), 147 (2022) (in Russian).
- [34] R.A. Castro Arata, L.V. Plotnikova, J.A. Salnikova, A.P. Smirnov, A.A. Kononov, O.S. Vezo, A.D. Garifullin, A.Yu. Kuvshinov, S.V. Voloshin, A.M. Polyanichko *Opt. spektr.***130**(6), 918 (2022) (in Russian).
- [35] V.T. Avanesyan, Zh.A. Salnikova. *AIP Conf. Proceed.*, **2308**, 030013 (2020). DOI: 10.1063/5.0035258
- [36] Zh.A. Salnikova, A.A. Kononov. *AIP Conf. Proceed.*, **2308**, 030017 (2020). DOI: 10.1063/5.0034028
- [37] *Description of the device „Novocontrol Concept–8I“* <https://ckpo.herzen.spb.ru/?page=dielectrici-oborudovanie&ID=5566>

- [38] Y.I. Frenkel. *Kineticheskaya Teoriya Zhidkostey* (Nauka, L., 1975) 592 p., (in Russian).
- [39] A.O. Vonti, A.V. Ilinsky, V.M. Kapralova, E.Yu. Shadrin. *ZhTF* **88**, 6 (934) (2018) (in Russian).
- [40] Yu.Ya. Gotlib, A.A. Darinskii, Yu.E. Svetlov, *Fizicheskaya kinetika makromolekul* (Khimiya, L., 1986) 272 p. (in Russian).
- [41] A.V. Finkelstein. *Fizika belkovykh molekul* (In-te of computer research, M.-Izhevsk, 2014), 424 p. (un Russian)
- [42] L.I. Krishtalik. *Biochim. Biophys. Acta (BBA) Bioenerg.*, **1273**, 139 (1996).
- [43] L.I. Kryshthalik. *UFN* **183**, 12 (1275) (2012) (in Russian).

*Translated by T.Zorina*